Accuracy of depth-integrated nonhydrostatic wave models

Gang Wang[1, 2], Jinhai Zheng [2*] and Qiuhua Liang[1, 3]

[1] Key Laboratory of Coastal Disaster and Defence (Hohai University), Ministry of Education, Nanjing 210098, China

[2] College of Harbour, Coastal and Offshore Engineering, Hohai University, Nanjing 210098, China

[3] School of Engineering, Newcastle University, Newcastle upon Tyne, United Kingdom NE1 7RU

Abstract: Depth-integrated nonhydrostatic models have been wildly used to simulate propagation of waves. Yet, there lacks a well-documented theoretical framework that can be used to assess the accuracy and scope of applications of these models and the related numerical approaches. In this work, we carry out Stokes-type Fourier and shoaling analyses to examine the linear and nonlinear properties of a popular one-layer depth-integrated nonhydrostatic model derived by Stelling and Zijlema (2003). The theoretical analysis shows that the model can satisfactorily interpret the dispersity for linear waves but presents evident divergence for nonlinear solutions even when $kd \to 0$. A generalized depth-integrated nonhydrostatic formulation using arbitrary elevation as a variable is then derived and analyzed to examine the effects of neglecting advective and diffusive nonlinear terms in the previous studies and explore possible improvements in numerical solutions for wave propagation. Compared with the previous studies, the new generalized formulation exhibits similar dispersion relationship and improved shoaling effect. However, no significant improvement is presented for the nonlinear properties, indicating that retaining neglected nonlinear terms may not significantly improve the nonlinear performance of the nonhydrostatic model. Further analysis shows that the nonlinear properties of the depth-integrated nonhydrostatic formulation may be improved by defining variables at one-third of the still water level. However, such an improvement comes at the price of decreasing accuracy in describing dispersion and shoaling properties.

Keywords: Nonhydrostatic models; surface gravity waves; depth-integrated models;

* Email address for correspondence: gangwang@hhu.edu.cn (G. Wang), jhzheng@hhu.edu.cn (J. Zheng)

dispersion relationship; nonlinear waves

1. Introduction

Numerical models have been widely used in the field of coastal engineering to simulate wave propagation from deep water to the surf zone. Nonhydrostatic models have been developed and widely reported in the literature to simulate free-surface water waves. These models are usually derived by depth-integrating the three-dimensional Reynolds averaged Navier-Stokes equations, providing governing equations that are relatively simple and analogous to the nonlinear shallow water equations with an addition of a vertical momentum equation and nonhydrostatic terms in the horizontal momentum equations. The simplified governing equations enable the use of simpler numerical schemes, leading to reduced computational cost. Furthermore, nonhydrostatic models usually adopt the spatially and temporally varying free surface motion as a single value function, and therefore require smaller vertical grids in comparison with the traditional free surface tracking approaches. This further improves their computational efficiency for large-scale wave transformation simulations.

The development of nonhydrostatic models can be traced back to Casulli and Stelling (1998) and their model defines the nonhydrostatic pressure at cell centers. As wave dispersion is usually described using the spatial derivatives of the nonhydrostatic pressure, imposing accurate pressure boundary condition at the free surface plays an important role in developing nonhydrostatic models. Stelling and Zijlema (2003) reported an accurate nonhydrostatic model, in which the Keller-box scheme was used to approximate the nonhydrostatic vertical pressure gradients at each vertical cell. Zijlema and Stelling (2005) subsequently reformulated the model with the terrain-following coordinates and employed a projection method to obtain the efficient and stable solutions. Their model has been released as an operational public domain code, known as SWASH (Zijlema et al., 2011). Algebraically representing the top-layer pressure using free-surface elevation and vertical acceleration, Yuan and Wu (2004) introduced a model that can effectively simulate wave propagation with a small number of vertical layers. Ahmadi et al. (2007) treated the top layer pressure

using an interpolation method, leading to significant improvement in the calculation of wave amplitude and phase. Young and Wu (2009) reported an effective approach to obtain the analytical pressure distribution at the top layer by introducing a Boussinesq-like formulation into their implicit nonhydrostatic model. Later on, Choi et al. (2011) presented an efficient curvilinear nonhydrostatic model for surface water waves, which adopted a higher order spline interpolation scheme to specify the pressure at the top-layer cells within a staggered grid framework.

In developing nonhydrostatic models, the fractional step procedure, i.e. the hydrostatic step and nonhydrostatic step, is usually employed to solve the depth-integrated nonhydrostatic shallow water equations. The nonhydrostatic pressure terms are dropped in the hydrostatic step and so the classical nonlinear shallow water equations are solved; the nonhydrostatic pressure effect is subsequently considered in the following nonhydrostatic step using most commonly a finite difference approach. Existing depth-integrated nonhydrostatic models mainly differ in the numerical approaches implemented the hydrostatic step, which may adopt the finite difference methods (Stelling and Zijlema, 2003), finite element methods (Walters, 2005; Wei and Jia, 2014) or finite-volume methods (Fang et al., 2015; Lu et al., 2015). Yamazaki et al. (2011) presented a depth-integrated, nonhydrostatic model for tsunami generation and propagation in the spherical coordinate system, implementing with a two-way grid-nesting upwind finite difference scheme. Aricò and Lo Re (2016) included convective acceleration terms in the vertical momentum equation, and claimed that the resulting nonhydrostatic model can better represent the strongly nonlinear processes.

Although the aforementioned models have been verified by numerical experiments to confirm their satisfactory solution accuracy, efficiency, and robustness in the simulation of dispersive surface gravity waves, there still lacks a comprehensive theoretical framework to precisely determine their application range. Lu et al. (2015) noted the numerical inaccuracy in wave phase and wave amplitude in their depth-integrated nonhydrostatic simulations, and declared that it was caused by the underestimation of wave dispersion and inaccurate calculation of linear vertical

profile of the nonhydrostatic pressure and velocity. However, the conclusion was not theoretically proved. Cui et al. (2014) and Zhu et al. (2014) attempted to explore model properties using more theoretically based methods. However, their investigations were limited to the analysis of linear dispersion. Preliminary attempt was also made by Bai and Cheung (2013) to derive a new multilayer formulation by integrating the continuity and Euler equations over each vertical layer and specify the model's application range through analysis of wave dispersion and nonlinearity.

This paper aims to re-derive rigorously the depth-integrated nonhydrostatic model and subsequently present a systematic analysis of the dispersion and nonlinearity properties of model to evaluate its merits and limitations. All advective and diffusive terms neglected in the previous studies are retained and assessed to examine whether the model can benefit from these additional terms. Rather than retaining more nonlinear terms, an alternative approach to improve the solution accuracy of a nonhydrostatic model is to use multiple layers in the vertical direction. However, multilayer models involve solving the Poisson equation and will dramatically increase the computational cost, hindering their wider applications. Therefore, the current paper focuses on the analysis of one-layer models, but the methodology may be extended to multiple layers and other models, such as NHWAVE (Ma et al., 2012), another readily accessible open source nonhydrostatic model.

The rest of the paper is organized as follows: Section 2 briefly reviews the continuity and Euler equations for describing free-surface fluid motions. Section 3 presents the detailed derivation of the depth-integrated, nonhydrostatic model proposed by Stelling and Zijlema (2003), and theoretically examines its linear and nonlinear wave properties; Section 4 derives a generalized set of one-layer, depth-integrated, nonhydrostatic formulations, where all terms neglected by Stelling and Zijlema (2003) are obtained, followed by the analysis and discussion of the linearity and nonlinearity characteristics of the new formulation. Finally, conclusions are drawn in Section 5.

2. Three-Dimensional Governing Equations

The irrotational flow of incompressible inviscid fluid can be described by the Euler equations

$$\frac{\partial u}{\partial t}+\frac{\partial u^2}{\partial x}+\frac{\partial uv}{\partial y}+\frac{\partial wu}{\partial z}=-g\frac{\partial \zeta}{\partial x}-\frac{1}{\rho}\frac{\partial q}{\partial x} \tag{1}$$

$$\frac{\partial v}{\partial t}+\frac{\partial uv}{\partial x}+\frac{\partial v^2}{\partial y}+\frac{\partial wv}{\partial z}=-g\frac{\partial \zeta}{\partial y}-\frac{1}{\rho}\frac{\partial q}{\partial y} \tag{2}$$

$$\frac{\partial w}{\partial t}+\frac{\partial uw}{\partial x}+\frac{\partial vw}{\partial y}+\frac{\partial w^2}{\partial z}=-\frac{1}{\rho}\frac{\partial q}{\partial z} \tag{3}$$

and the corresponding continuity equation

$$\frac{\partial u}{\partial x}+\frac{\partial v}{\partial y}+\frac{\partial w}{\partial z}=0 \tag{4}$$

Herein, t is time; x, y and z are the three Cartesian coordinate components; u, v and w are the velocity components in the three Cartesian directions; ζ denotes the free surface elevation from the still water level; g and ρ are respectively the acceleration due to gravity and the fluid density; q is the nonhydrostatic pressure components and consequently the total pressure p is given by

$$p=\rho g\left(\zeta-z\right)+q \tag{5}$$

As the fluid is bounded by the sea bottom and a free surface, the dynamic and kinematic boundary conditions apply, where

$$q_\zeta=0 \qquad \text{at } z=\zeta \tag{6}$$

$$w_\zeta=\frac{\partial \zeta}{\partial t}+u_\zeta\frac{\partial \zeta}{\partial x}+v_\zeta\frac{\partial \zeta}{\partial y} \qquad \text{at } z=\zeta \tag{7}$$

The bottom boundary condition requires

$$w_{-d}=-u_{-d}\frac{\partial d}{\partial x}-v_{-d}\frac{\partial d}{\partial y} \tag{8}$$

in which the subscript d indicates the variable at the bottom.

3. Depth-Integrated, Nonhydrostatic Model of Stelling and Zijlema (2003)

In this section the depth-integrated nonhydrostatic model proposed by Stelling and Zijlema (2003) is re-derived, followed by the analysis of its linear and nonlinear properties.

3.1 Derivation of the governing equations

Assuming the velocity and pressure vary linearly in the vertical direction, the model

incorporated with the Keller-box method may be expressed as

$$u = u_{-d} + \frac{z+d}{h}\left(u_{\zeta} - u_{-d}\right) \tag{9}$$

$$v = v_{-d} + \frac{z+d}{h}\left(v_{\zeta} - v_{-d}\right) \tag{10}$$

$$w = w_{-d} + \frac{z+d}{h}\left(w_{\zeta} - w_{-d}\right) \tag{11}$$

and

$$q = \frac{\zeta - z}{h} q_{-d} \tag{12}$$

where $h = \zeta + d$ defines the flow depth; and the subscripts ζ and $-d$ denote the variables defined at the free surface and the bottom, respectively.

Integrating the continuity equation (4) from the bottom to the free surface and using the Leibniz rule leads to

$$\frac{\partial}{\partial x}\int_{-d}^{\zeta} u\mathrm{d}z + \frac{\partial}{\partial y}\int_{-d}^{\zeta} v\mathrm{d}z + w_{\zeta} - u_{\zeta}\frac{\partial \zeta}{\partial x} - v_{\zeta}\frac{\partial \zeta}{\partial y} - w_{-d} - u_{-d}\frac{\partial d}{\partial x} - v_{-d}\frac{\partial d}{\partial y} = 0 \tag{13}$$

Applying the kinematic condition (7) and the bottom condition (8) gives

$$\frac{\partial \zeta}{\partial t} + \frac{\partial h\bar{u}}{\partial x} + \frac{\partial h\bar{v}}{\partial y} = 0 \tag{14}$$

with the depth-integrated horizontal velocities $\bar{u}$ and $\bar{v}$ defined as

$$\bar{u} = \frac{1}{h}\int_{-d}^{\zeta} u\mathrm{d}z \tag{15}$$

and

$$\bar{v} = \frac{1}{h}\int_{-d}^{\zeta} v\mathrm{d}z \tag{16}$$

As $\bar{u}$ and $\bar{v}$ are assumed to vary linearly in the vertical direction, they are essentially the middle-depth velocities.

With the kinematic conditions (6) and (7) and the bottom condition (8), the horizontal momentum equation (1) may be integrated over the total water depth to give

$$\frac{\partial h\bar{u}}{\partial t} + \frac{\partial}{\partial x}\int_{-d}^{\zeta} u^2\mathrm{d}z + \frac{\partial}{\partial y}\int_{-d}^{\zeta} uv\mathrm{d}z = -gh\frac{\partial \zeta}{\partial x} - \frac{h}{2\rho}\frac{\partial q_{-d}}{\partial x} - \frac{q_{-d}}{2\rho}\frac{\partial\left(\zeta - d\right)}{\partial x} \tag{17}$$

where the Leibniz rule has also been applied.

The integrals of the nonlinear terms in Eq. (17) may be obtained from Eqs. (9) and (10), i.e.

$$\int_{-d}^{\zeta} u^2 \mathrm{d}z = h\bar{u}^2 + \frac{h}{12}\left(u_{\zeta} - u_{-d}\right)^2 \tag{18}$$

and

$$\int_{-d}^{\zeta} uv \mathrm{d}z = h\bar{u}\bar{v} + \frac{h}{12}\left(u_{\zeta} - u_{-d}\right)\left(v_{\zeta} - v_{-d}\right) \tag{19}$$

The second terms in the right-hand side of Eqs. (18) and (19) are the dispersion terms resulting from the vertical non-uniformities of the flow velocity. These terms are considered to be diffusion in common practice and directly neglected in the model reported by Stelling and Zijlema (2003).

Substituting the dispersion-free (i.e. neglecting the dispersion terms) Eqs. (18) and (19) into Eq. (17), the *x*-direction depth-integrated momentum equation is derived

$$\frac{\partial h\bar{u}}{\partial t} + \frac{\partial h\bar{u}^2}{\partial x} + \frac{\partial h\bar{u}\bar{v}}{\partial y} + gh\frac{\partial \zeta}{\partial x} + \frac{h}{2\rho}\frac{\partial q_{-d}}{\partial x} + \frac{q_{-d}}{2\rho}\frac{\partial\left(\zeta - d\right)}{\partial x} = 0 \tag{20}$$

Similarly, the *y*-direction and *w*-direction momentum equations can be derived from Eqs. (2) and (3):

$$\frac{\partial h\bar{v}}{\partial t} + \frac{\partial h\bar{u}\bar{v}}{\partial x} + \frac{\partial h\bar{v}^2}{\partial y} + gh\frac{\partial \zeta}{\partial y} + \frac{h}{2\rho}\frac{\partial q_{-d}}{\partial y} + \frac{q_{-d}}{2\rho}\frac{\partial\left(\zeta - d\right)}{\partial y} = 0 \tag{21}$$

and

$$\frac{\partial h\bar{w}}{\partial t} + \frac{\partial h\bar{u}\bar{w}}{\partial x} + \frac{\partial h\bar{v}\bar{w}}{\partial y} - \frac{q_{-d}}{\rho} = 0 \tag{22}$$

where $\bar{w} = \left(w_{\zeta} + w_{-d}\right)/2$ is the depth-integrated vertical velocity. Stelling and Zijlema (2003) concluded that the second and third terms in Eq. (22) are the advective and diffusive terms and may be neglected as they are generally small compared to the vertical acceleration and can be instantaneously determined by the nonhydrostatic pressure gradient. So, the above equation may be approximated as

$$\frac{\partial \bar{w}}{\partial t} - \frac{q_{-d}}{h\rho} = 0 \tag{23}$$

Neglect of the dispersion terms in Eqs. (20) and (21) and the advective and diffusive terms in Eq. (23) has been initially considered as the main reason as why the Stelling and Zijlema (2003) model cannot predict accurately the nonlinear waveforms even in the shallow water. Aricò and Lo Re (2016) retained the convective terms in the vertical momentum equations and solved Eq. (22) instead of Eq. (23) in their model.

They declared that the resulting model matched the measured data better than the model without vertical convective terms, especially for strongly nonlinear waves. However, no theoretical validation was presented to support their conclusion.

The continuity equation (4) may be approximated as the conservation of local mass, which yields

$$\frac{\partial \overline{u}}{\partial x}+\frac{\partial \overline{v}}{\partial y}+\frac{w_{\zeta}-w_{-d}}{h}=0 \tag{24}$$

The bottom condition (8) is approximated to become

$$w_{-d}=-\overline{u}\frac{\partial d}{\partial x}-\overline{v}\frac{\partial d}{\partial y} \tag{25}$$

This essentially uses the depth-integrated velocities to represent the velocities at the bottom, which may introduce model error for the shoaling effect.

As a summary, Eqs. (14), (20), (21), (23) and (24) are the governing equations of the considered depth-integrated nonhydrostatic model for free-surface water waves, and Eq. (25) is the corresponding boundary condition.

3.2 Linear and nonlinear characteristics

Stoke-type Fourier analysis enables extraction of the linear and nonlinear quantities embodied in the formulation derived above. The variables are approximated as power series, giving as follows

$$\zeta=\varepsilon a^{(1)}\cos(kx-\omega t)+\varepsilon^2 a^{(2)}\cos 2(kx-\omega t)+\varepsilon^3 a^{(3)}\cos 3(kx-\omega t) \tag{26}$$

$$\overline{u}=\varepsilon U^{(1)}\cos(kx-\omega t)+\varepsilon^2 U^{(2)}\cos 2(kx-\omega t)+\varepsilon^3 U^{(3)}\cos 3(kx-\omega t) \tag{27}$$

$$w_s=\varepsilon W_s^{(1)}\sin(kx-\omega t)+\varepsilon^2 W_s^{(2)}\sin 2(kx-\omega t)+\varepsilon^3 W_s^{(3)}\sin 3(kx-\omega t) \tag{28}$$

$$w_{-d}=\varepsilon W_{-d}^{(1)}\sin(kx-\omega t)+\varepsilon^2 W_{-d}^{(2)}\sin 2(kx-\omega t)+\varepsilon^3 W_{-d}^{(3)}\sin 3(kx-\omega t) \tag{29}$$

$$p_{-d}=\varepsilon P^{(1)}\cos(kx-\omega t)+\varepsilon^2 P^{(2)}\cos 2(kx-\omega t)+\varepsilon^3 P^{(3)}\cos 3(kx-\omega t) \tag{30}$$

where the small perturbation parameter ε may be commonly considered as the wave slope defined as $\varepsilon = ka$ with k and a respectively being the wavenumber amplitude; $a^{(i)}$, $U^{(i)}$, $W_s^{(i)}$, $W_{-d}^{(i)}$, $p^{(i)}$ are real functions; ω is the circular frequency; and the superscripts 1, 2 and 3 denote the first-, second- and third-order solutions, respectively. In order to avoid singular unbounded solutions at the third order, the frequency and

first order solutions are expanded

$$\omega = \omega\left(1+\varepsilon^2\omega^{(13)}\right),\quad U^{(1)} = U^{(1)}\left(1+\varepsilon^2 U^{(13)}\right),\quad W_s^{(1)} = W_s^{(1)}\left(1+\varepsilon^2 W_s^{(13)}\right),$$
$$W_{-d}^{(1)} = W_{-d}^{(1)}\left(1+\varepsilon^2 W_{-d}^{(13)}\right),\quad p^{(1)} = p^{(1)}\left(1+\varepsilon^2 p^{(13)}\right) \tag{31}$$

Substituting Eqs. (26) - (31) into the one-dimensional governing equations (14), (20), (23) - (25) yields the linear solutions for their first order system

$$\omega^2 = gk\frac{kd}{1+k^2d^2/4} \tag{32}$$

$$U^{(1)} = a^{(1)}\omega\frac{4+k^2d^2}{4kd+k^3d^3} \tag{33}$$

$$W_s^{(1)} = a^{(1)}\omega \tag{34}$$

$$W_{-d}^{(1)} = 0 \tag{35}$$

$$P^{(1)} = -\rho g a^{(1)}\frac{2k^2d^2}{4+k^2d^2} \tag{36}$$

As the "deep-water" depth limitation corresponds to $kd = \pi$, we compare the phase speed with the one given by the Airy linear-theory for the range $0 \le kd \le \pi$, and a maximum difference of less than 5% is observed for the entire range, as shown in Figure 1.

Substituting Eqs. (26) - (31) into the governing equations (14), (20), (23) - (25) and collecting the second and third order terms of $O(\varepsilon^2)$ and $O(\varepsilon^3)$ lead to the second- and third-order solutions, with the second- and third-order nonlinear amplitudes given as

$$a_{\mathrm{S\&Z}}^{(2)} = \frac{3a^{(1)2}}{4k^2d^3}\left(\frac{4}{3}+\frac{1}{9}k^2d^2\right) \tag{37}$$

and

$$a_{\mathrm{S\&Z}}^{(3)} = \frac{27}{64}\frac{a^{(1)3}}{k^4d^6}\left(\frac{28}{27}-\frac{4}{27}k^2d^2\right) \tag{38}$$

Herein we focus on the comparison of $a^{(2)}$ and $a^{(3)}$ with the Stokes second- and third-order solutions (Svendsen, 2006), given as follows

$$a_{\mathrm{Stokes}}^{(2)} = \frac{ka^{(1)2}}{4}\frac{\cosh kd\left(2\cosh^2 kd+1\right)}{\sinh^3 kd} \tag{39}$$

$$a_{\mathrm{Stokes}}^{(3)} = k^2a^{(1)3}\frac{3\left(8\cosh^6 kd+1\right)}{64\sinh^6 kd} \tag{40}$$

which are expanded from $kd = 0$ to become

$$a_{\text{Stokes}}^{(2)} = \frac{3a^{(1)2}}{4k^2d^3}\left[1+\frac{2}{3}k^2d^2+\frac{7}{45}k^4d^4+\mathrm{O}\left(k^6d^6\right)\right] \tag{41}$$

$$a_{\text{Stokes}}^{(3)} = \frac{27}{64}\frac{a^{(1)3}}{k^4d^6}\left[1+\frac{5}{3}k^2d^2+\frac{64}{45}k^4d^4++\mathrm{O}\left(k^6d^6\right)\right] \tag{42}$$

Apparently, $a_{\text{S\&Z}}^{(2)}$ and $a_{\text{S\&Z}}^{(3)}$ do not match the Stokes theory in shallow water. The one-layer depth-integrated nonhydrostatic model derived by Stelling and Zijlema (2003) overestimates 1/3 of the second-order solutions and 1/27 of the third-order solutions in comparison with the exact Stokes solutions for $kd \rightarrow 0$. Figure 2 shows the nonlinear solutions normalized by the Stokes solutions over the range of $0 \leq kd \leq \pi$. The normalized second- and third-order solutions are observed to monotonically decrease. The second-order solution overestimates and underestimates the nonlinearity in the range of $0 \leq kd \leq 1$ and $kd > 1$, respectively. The third order solution approaches the exact Stokes solution for $kd < 0.14$ (with a maximum error of 1/27 at $kd \rightarrow 0$), followed by an underestimation of the exact solution beyond this range. The underestimated nonlinear results will lead to the smaller amplitude of waves traveling in the intermediate and deep water.

In free-surface wave propagation, the wave amplitude usually increases as the water depth decreases towards the shore, known as shoaling effect. This is one of the fundamental properties embedded in the governing equations for wave traveling over varying depth. Herein, the linear shoaling gradient describing the amplitude varying over a constant slope is compared with the result derived by Madsen and Sørensen (1992) using the energy flux conservation combined with Stokes linear theory. The linearized horizontal one-dimensional governing equations (14), (20), (22) - (24) together with the boundary condition (25) may be converted into a Boussinesq-type formulation by retaining the terms of first-order of bottom slope, given as

$$\frac{\partial \zeta}{\partial t} + d\frac{\partial \bar{u}}{\partial x} + \bar{u}\frac{\partial d}{\partial x} = 0 \tag{43}$$

and

$$\frac{\partial \bar{u}}{\partial t} + g\frac{\partial \zeta}{\partial x} - \frac{3}{4}d\frac{\partial d}{\partial x}\frac{\partial^2 \bar{u}}{\partial t \partial x} - \frac{1}{4}d^2\frac{\partial^3 \bar{u}}{\partial t \partial^2 x} = 0 \tag{44}$$

Following the procedure adopted by Madsen and Sørensen (1992), we seek solutions

of the following form:

$$\zeta(x,t) = Ae^{i\left(\omega t - \int k(x)dx\right)} \tag{45}$$

$$u(x,t) = \left[D(x) + i\tilde{D}_x(x)\right]e^{i\left(\omega t - \int k(x)dx\right)} \tag{46}$$

where i is the imaginary unit, $\tilde{D}_x$ is introduced to account for the small phase resulting from a slowly varying bottom. Substituting Eqs. (45) -(46) into Eqs. (43) -(44) and collecting the terms in the real and imaginary parts yield

$$\frac{A_x}{A} = -s^{\text{S\&Z}}\frac{d_x}{d} \tag{47}$$

where $s^{\text{S\&Z}}$ is the shoaling gradient, reading as

$$s^{\text{S\&Z}} = \left(\frac{1}{4} - \frac{3}{16}k^2d^2\right) \tag{48}$$

Figure 3 shows that the depth-integrated nonhydrostatic model agrees closely with the exact solution for $kd \leq 1.1$, and then diverges monotonically from the exact solution for $kd > 1.1$. The model underestimates the amplitude at large negative shoaling gradients, although the discrepancy should only correspond to secondary effects in the intermediate- and deep-water conditions when the wave amplitude is less sensitive to the shoaling process.

4 Generalized one-layer Depth-Integrated Nonhydrostatic Model

4.1 Derivation of the governing equations

In this section, we use the Taylor-series-type expansion to relate the different velocity variables, and derive a new one-layer depth-integrated nonhydrostatic model. In contrast to the model of Stelling and Zijlema (2003), all nonlinear terms in the momentum equations are retained, together with accurate description of the bottom condition. The dispersion relationship, shoaling gradients and the second- and third-order harmonic solutions of the generalized model are derived and compared with the model of Stelling and Zijlema (2003) and Stokes wave theories.

The velocities and nonhydrostatic pressure is assumed linearly varying and given as

$$u = u_{z\alpha} + \left(z - z_\alpha\right)\left(\frac{\partial u}{\partial z}\right)_{z\alpha} + \cdots \tag{49}$$

$$v = v_{z\alpha} + \left(z - z_\alpha\right)\left(\frac{\partial v}{\partial z}\right)_{z\alpha} + \cdots \tag{50}$$

$$w = w_{z\alpha} + \left(z - z_\alpha\right)\left(\frac{\partial w}{\partial z}\right)_{z\alpha} + \cdots \tag{51}$$

$$q = q_{z\alpha} + \left(z - z_\alpha\right)\left(\frac{\partial q}{\partial z}\right)_{z\alpha} + \cdots \tag{52}$$

where the flow variables, $u_{z\alpha}$, $v_{z\alpha}$, $w_{z\alpha}$ and $q_{z\alpha}$, are defined at an arbitrary elevation z_α:

$$z_\alpha = -\alpha d \tag{53}$$

where $0 \le \alpha \le 1$, with $\alpha = 0$ or 1 defining the variables at the still water level or the bottom and $\alpha = 1/2$ giving the depth-integrated variables. Assuming inviscid fluids, the irrotational conditions apply and are given as follows

$$\frac{\partial u}{\partial z} = \frac{\partial w}{\partial x}, \frac{\partial v}{\partial z} = \frac{\partial w}{\partial y}, \frac{\partial u}{\partial y} = \frac{\partial v}{\partial x} \tag{54}$$

Using the irrotationality conditions in (54), Eq. (49) may be rewritten as

$$u = u_{z\alpha} + \left(z - z_\alpha\right)\left(\frac{\partial w}{\partial x}\right)_{z\alpha} + \cdots \tag{55}$$

Similarly, the expressions for the horizontal velocity component v, the vertical velocity component w and the pressure q can be obtained:

$$v = v_{z\alpha} + \left(z - z_\alpha\right)\left(\frac{\partial w}{\partial y}\right)_{z\alpha} + \cdots \tag{56}$$

$$w = w_{z\alpha} - \left(z - z_\alpha\right)\left(\frac{\partial u}{\partial x} + \frac{\partial v}{\partial y}\right)_{z\alpha} + \cdots \tag{57}$$

$$q = q_{z\alpha} - \rho\left(z - z_\alpha\right)\left[\frac{\partial w_{z\alpha}}{\partial t} + u_{z\alpha}\left(\frac{\partial w}{\partial x}\right)_{z\alpha} + v_{z\alpha}\left(\frac{\partial w}{\partial y}\right)_{z\alpha} - w_{z\alpha}\left(\frac{\partial u}{\partial x}\right)_{z\alpha} - w_{z\alpha}\left(\frac{\partial v}{\partial y}\right)_{z\alpha}\right] + \cdots \tag{58}$$

where the continuity equation (4) and the irrotational conditions (54) have been applied.

The partial derivatives in Eqs. (55) - (58) may be expressed using the variables at elevation z_α and become

$$\left(\frac{\partial w}{\partial x}\right)_{z\alpha} = \frac{\partial w_{z\alpha}}{\partial x} + \frac{\partial z_\alpha}{\partial x}\left(\frac{\partial u}{\partial x} + \frac{\partial v}{\partial y}\right)_{z\alpha} \tag{59}$$

$$\left(\frac{\partial w}{\partial y}\right)_{z\alpha} = \frac{\partial w_{z\alpha}}{\partial y} + \frac{\partial z_\alpha}{\partial y}\left(\frac{\partial u}{\partial x} + \frac{\partial v}{\partial y}\right)_{z\alpha} \tag{60}$$

$$\left(\frac{\partial u}{\partial x}\right)_{z\alpha} = \frac{\partial u_{z\alpha}}{\partial x} - \frac{\partial z_\alpha}{\partial x}\left(\frac{\partial w}{\partial x}\right)_{z\alpha} \tag{61}$$

$$\left(\frac{\partial v}{\partial y}\right)_{z\alpha} = \frac{\partial v_{z\alpha}}{\partial y} - \frac{\partial z_\alpha}{\partial y}\left(\frac{\partial w}{\partial y}\right)_{z\alpha} \tag{62}$$

leading to

$$\left(\frac{\partial w}{\partial x}\right)_{z\alpha} = \frac{\partial w_{z\alpha}}{\partial x} + \frac{\partial z_\alpha}{\partial x}\left(\frac{\partial u_{z\alpha}}{\partial x} + \frac{\partial v_{z\alpha}}{\partial y}\right) + O\left[\left(\frac{\partial z_\alpha}{\partial x}\right)^2, \frac{\partial z_\alpha}{\partial x}\frac{\partial z_\alpha}{\partial y}, \left(\frac{\partial z_\alpha}{\partial y}\right)^2\right] \tag{63}$$

$$\left(\frac{\partial w}{\partial y}\right)_{z\alpha} = \frac{\partial w_{z\alpha}}{\partial y} + \frac{\partial z_\alpha}{\partial y}\left(\frac{\partial u_{z\alpha}}{\partial x} + \frac{\partial v_{z\alpha}}{\partial y}\right) + O\left[\left(\frac{\partial z_\alpha}{\partial x}\right)^2, \frac{\partial z_\alpha}{\partial x}\frac{\partial z_\alpha}{\partial y}, \left(\frac{\partial z_\alpha}{\partial y}\right)^2\right] \tag{64}$$

$$\left(\frac{\partial u}{\partial x}\right)_{z\alpha} = \frac{\partial u_{z\alpha}}{\partial x} - \frac{\partial z_\alpha}{\partial x}\frac{\partial w_{z\alpha}}{\partial x} + O\left[\left(\frac{\partial z_\alpha}{\partial x}\right)^2\right] \tag{65}$$

$$\left(\frac{\partial v}{\partial y}\right)_{z\alpha} = \frac{\partial v_{z\alpha}}{\partial y} - \frac{\partial z_\alpha}{\partial y}\frac{\partial w_{z\alpha}}{\partial y} + O\left[\left(\frac{\partial z_\alpha}{\partial y}\right)^2\right] \tag{66}$$

In the above derivation, the products of the horizontal bottom gradients are neglected, indicating that the resulting formulation is restricted to applications with slowly varying bottom.

Subsequently, the velocities and nonhydrostatic pressure can be expressed as

$$u = u_{z\alpha} + \left(z - z_\alpha\right)\left[\frac{\partial w_{z\alpha}}{\partial x} + \frac{\partial z_\alpha}{\partial x}\left(\frac{\partial u_{z\alpha}}{\partial x} + \frac{\partial v_{z\alpha}}{\partial y}\right)\right] + \cdots \tag{67}$$

$$v = v_{z\alpha} + \left(z - z_\alpha\right)\left[\frac{\partial w_{z\alpha}}{\partial y} + \frac{\partial z_\alpha}{\partial y}\left(\frac{\partial u_{z\alpha}}{\partial x} + \frac{\partial v_{z\alpha}}{\partial y}\right)\right] + \cdots \tag{68}$$

$$w = w_{z\alpha} - \left(z - z_\alpha\right)\left(\frac{\partial u_{z\alpha}}{\partial x} + \frac{\partial v_{z\alpha}}{\partial y} - \frac{\partial z_\alpha}{\partial x}\frac{\partial w_{z\alpha}}{\partial x} - \frac{\partial z_\alpha}{\partial y}\frac{\partial w_{z\alpha}}{\partial y}\right) + \cdots \tag{69}$$

$$q = q_{z\alpha} - \rho\left(z - z_\alpha\right)\left[\begin{array}{l} \dfrac{\partial w_{z\alpha}}{\partial t} + u_{z\alpha}\dfrac{\partial w_{z\alpha}}{\partial x} + v_{z\alpha}\dfrac{\partial w_{z\alpha}}{\partial y} - w_{z\alpha}\dfrac{\partial u_{z\alpha}}{\partial x} - w_{z\alpha}\dfrac{\partial v_{z\alpha}}{\partial y} \\ + \dfrac{\partial z_\alpha}{\partial x}\left[w_{z\alpha}\dfrac{\partial w_{z\alpha}}{\partial x} + u_{z\alpha}\left(\dfrac{\partial u_{z\alpha}}{\partial x} + \dfrac{\partial v_{z\alpha}}{\partial y}\right)\right] \\ + \dfrac{\partial z_\alpha}{\partial y}\left[w_{z\alpha}\dfrac{\partial w_{z\alpha}}{\partial y} + v_{z\alpha}\left(\dfrac{\partial u_{z\alpha}}{\partial x} + \dfrac{\partial v_{z\alpha}}{\partial y}\right)\right] \end{array}\right] + \cdots \tag{70}$$

The dynamic boundary condition (6) is reformulated as

$$q_{z\alpha}=\rho\left(\zeta-z_\alpha\right)\left[\begin{array}{l}\dfrac{\partial w_{z\alpha}}{\partial t}+u_{z\alpha}\dfrac{\partial w_{z\alpha}}{\partial x}+v_{z\alpha}\dfrac{\partial w_{z\alpha}}{\partial y}-w_{z\alpha}\dfrac{\partial u_{z\alpha}}{\partial x}-w_{z\alpha}\dfrac{\partial v_{z\alpha}}{\partial y}\\ +\dfrac{\partial z_\alpha}{\partial x}\left[w_{z\alpha}\dfrac{\partial w_{z\alpha}}{\partial x}+u_{z\alpha}\left(\dfrac{\partial u_{z\alpha}}{\partial x}+\dfrac{\partial v_{z\alpha}}{\partial y}\right)\right]\\ +\dfrac{\partial z_\alpha}{\partial y}\left[w_{z\alpha}\dfrac{\partial w_{z\alpha}}{\partial y}+v_{z\alpha}\left(\dfrac{\partial u_{z\alpha}}{\partial x}+\dfrac{\partial v_{z\alpha}}{\partial y}\right)\right]\end{array}\right] \tag{71}$$

The bottom condition (8) may be expressed as

$$\begin{aligned}&w_{z\alpha}+u_{z\alpha}\frac{\partial d}{\partial x}+v_{z\alpha}\frac{\partial d}{\partial y}\\&=\left(d+z_\alpha\right)\left\{-\frac{\partial u_{z\alpha}}{\partial x}-\frac{\partial v_{z\alpha}}{\partial y}+\frac{\partial z_\alpha}{\partial x}\frac{\partial w_{z\alpha}}{\partial x}+\frac{\partial z_\alpha}{\partial y}\frac{\partial w_{z\alpha}}{\partial y}+\right.\\&\left.\left[\frac{\partial w_{z\alpha}}{\partial x}+\frac{\partial z_\alpha}{\partial x}\left(\frac{\partial u_{z\alpha}}{\partial x}+\frac{\partial v_{z\alpha}}{\partial y}\right)\right]\frac{\partial d}{\partial x}+\left[\frac{\partial w_{z\alpha}}{\partial y}+\frac{\partial z_\alpha}{\partial y}\left(\frac{\partial u_{z\alpha}}{\partial x}+\frac{\partial v_{z\alpha}}{\partial y}\right)\right]\frac{\partial d}{\partial y}\right\}\end{aligned} \tag{72}$$

Integrating the continuity equation (4) from the bottom to the free surface, applying the Leibniz rule, and combining the kinematic condition (7) and the bottom condition (8), we finally have the following equation

$$\begin{aligned}&\frac{\partial\zeta}{\partial t}+\frac{\partial hu_{z\alpha}}{\partial x}+\frac{\partial hv_{z\alpha}}{\partial y}=-\frac{1}{2}\frac{\partial}{\partial x}\left\{h\left(\zeta-2z_\alpha-d\right)\left[\frac{\partial w_{z\alpha}}{\partial x}+\frac{\partial z_\alpha}{\partial x}\left(\frac{\partial u_{z\alpha}}{\partial x}+\frac{\partial v_{z\alpha}}{\partial y}\right)\right]\right\}\\&-\frac{1}{2}\frac{\partial}{\partial y}\left\{h\left(\zeta-2z_\alpha-d\right)\left[\frac{\partial w_{z\alpha}}{\partial y}+\frac{\partial z_\alpha}{\partial y}\left(\frac{\partial u_{z\alpha}}{\partial x}+\frac{\partial v_{z\alpha}}{\partial y}\right)\right]\right\}=0\end{aligned} \tag{73}$$

Compared with Eq. (14), the above equation contains additional frequency dispersion terms in the right-hand side. Apparently, these additional terms will vanish if depth-integrated velocities are used, i.e. when $z_\alpha = (\zeta + d)/2$.

Integrating the horizontal momentum equation (1) from the seabed to the free surface and applying the boundary conditions in (6) - (8) will give

$$\frac{\partial hu_{z\alpha}}{\partial t}+\frac{\partial hu_{z\alpha}^2}{\partial x}+\frac{\partial hu_{z\alpha}v_{z\alpha}}{\partial y}+gh\frac{\partial\zeta}{\partial x}+\frac{1}{2\rho}\frac{\partial}{\partial x}\left(\frac{h^2q_{z\alpha}}{\zeta-z_\alpha}\right)-\frac{hq_{z\alpha}}{\rho\left(\zeta-z_\alpha\right)}\frac{\partial d}{\partial x}=\Lambda_{x1}+\Lambda_{x2} \tag{74}$$

where

$$\Lambda_{x1}=-\frac{1}{2}\left\{h\left(\zeta-2z_\alpha-d\right)\left[\frac{\partial w_{z\alpha}}{\partial x}+\frac{\partial z_\alpha}{\partial x}\left(\frac{\partial u_{z\alpha}}{\partial x}+\frac{\partial v_{z\alpha}}{\partial y}\right)\right]\right\}_t$$
$$-u_{z\alpha}\left\{h\left(\zeta-2z_\alpha-d\right)\left[\frac{\partial w_{z\alpha}}{\partial x}+\frac{\partial z_\alpha}{\partial x}\left(\frac{\partial u_{z\alpha}}{\partial x}+\frac{\partial v_{z\alpha}}{\partial y}\right)\right]\right\}_x-v_{z\alpha}\left\{h\left(\zeta-2z_\alpha-d\right)\left[\frac{\partial w_{z\alpha}}{\partial x}+\frac{\partial z_\alpha}{\partial x}\left(\frac{\partial u_{z\alpha}}{\partial x}+\frac{\partial v_{z\alpha}}{\partial y}\right)\right]\right\}_y$$
$$-\frac{h}{2}\left(\zeta-2z_\alpha-d\right)\left[\frac{\partial w_{z\alpha}}{\partial x}+\frac{\partial z_\alpha}{\partial x}\left(\frac{\partial u_{z\alpha}}{\partial x}+\frac{\partial v_{z\alpha}}{\partial y}\right)\right]\left(\frac{\partial u_{z\alpha}}{\partial x}+\frac{\partial v_{z\alpha}}{\partial y}\right)$$
$$-\frac{h}{2}\left(\zeta-2z_\alpha-d\right)\left\{\left[\frac{\partial w_{z\alpha}}{\partial x}+\frac{\partial z_\alpha}{\partial x}\left(\frac{\partial u_{z\alpha}}{\partial x}+\frac{\partial v_{z\alpha}}{\partial y}\right)\right]\frac{\partial u_{z\alpha}}{\partial x}+\left[\frac{\partial w_{z\alpha}}{\partial y}+\frac{\partial z_\alpha}{\partial y}\left(\frac{\partial u_{z\alpha}}{\partial x}+\frac{\partial v_{z\alpha}}{\partial y}\right)\right]\frac{\partial u_{z\alpha}}{\partial y}\right\} \tag{75}$$

and

$$\Lambda_{x2}=-\frac{1}{3}\left\{\left[\left(\zeta-z_\alpha\right)^3+\left(d+z_\alpha\right)^3\right]\left[\frac{\partial w_{z\alpha}}{\partial x}+\frac{\partial z_\alpha}{\partial x}\left(\frac{\partial u_{z\alpha}}{\partial x}+\frac{\partial v_{z\alpha}}{\partial y}\right)\right]^2\right\}_x$$
$$-\frac{1}{3}\left\{\left[\left(\zeta-z_\alpha\right)^3+\left(d+z_\alpha\right)^3\right]\left[\frac{\partial w_{z\alpha}}{\partial x}+\frac{\partial z_\alpha}{\partial x}\left(\frac{\partial u_{z\alpha}}{\partial x}+\frac{\partial v_{z\alpha}}{\partial y}\right)\right]\left[\frac{\partial w_{z\alpha}}{\partial y}+\frac{\partial z_\alpha}{\partial y}\left(\frac{\partial u_{z\alpha}}{\partial x}+\frac{\partial v_{z\alpha}}{\partial y}\right)\right]\right\}_y \tag{76}$$

All the terms neglected in the model of Stelling and Zijlema (2003) have been retained and contained in the two additional terms Λ_{x1} and Λ_{x2} appeared on the right hand side of Eq. (74). All dispersion and nonlinear terms in Λ_{x1} are related to ($\zeta - 2z_\alpha$ - d), which arise from the definition of velocities at z_α and will vanish with the use of depth-integrated velocities. All terms in Λ_{x2} contain $(\zeta - z_\alpha)^3 + (d + z_\alpha)^3$ and are essentially the neglected dispersion terms in Eqs. (18) - (19). These additional terms together with the optimization of α are expected to improve linear and nonlinear properties of the new formulation.

The v-momentum equation (2) can be similarly derived

$$\frac{\partial hv_{z\alpha}}{\partial t}+\frac{\partial hu_{z\alpha v_{z\alpha}}}{\partial x}+\frac{\partial hv_{z\alpha}^2}{\partial y}+gh\frac{\partial\zeta}{\partial y}+\frac{1}{2\rho}\frac{\partial}{\partial y}\left(\frac{h^2q_{z\alpha}}{\zeta-z_\alpha}\right)-\frac{hq_{z\alpha}}{\rho\left(\zeta-z_\alpha\right)}\frac{\partial d}{\partial y}=\Lambda_{1y}+\Lambda_{1y} \tag{77}$$

where

$$\Lambda_{y1}=-\frac{1}{2}\left\{h\left(\zeta-2z_\alpha-d\right)\left[\frac{\partial w_{z\alpha}}{\partial y}+\frac{\partial z_\alpha}{\partial y}\left(\frac{\partial u_{z\alpha}}{\partial x}+\frac{\partial v_{z\alpha}}{\partial y}\right)\right]\right\}_t$$
$$-u_{z\alpha}\left\{h\left(\zeta-2z_\alpha-d\right)\left[\frac{\partial w_{z\alpha}}{\partial y}+\frac{\partial z_\alpha}{\partial y}\left(\frac{\partial u_{z\alpha}}{\partial x}+\frac{\partial v_{z\alpha}}{\partial y}\right)\right]\right\}_x-v_{z\alpha}\left\{h\left(\zeta-2z_\alpha-d\right)\left[\frac{\partial w_{z\alpha}}{\partial y}+\frac{\partial z_\alpha}{\partial y}\left(\frac{\partial u_{z\alpha}}{\partial x}+\frac{\partial v_{z\alpha}}{\partial y}\right)\right]\right\}_y$$
$$-\frac{h}{2}\left(\zeta-2z_\alpha-d\right)\left[\frac{\partial w_{z\alpha}}{\partial y}+\frac{\partial z_\alpha}{\partial y}\left(\frac{\partial u_{z\alpha}}{\partial x}+\frac{\partial v_{z\alpha}}{\partial y}\right)\right]\left(\frac{\partial u_{z\alpha}}{\partial x}+\frac{\partial v_{z\alpha}}{\partial y}\right)$$
$$-\frac{h}{2}\left(\zeta-2z_\alpha-d\right)\left\{\left[\frac{\partial w_{z\alpha}}{\partial y}+\frac{\partial z_\alpha}{\partial y}\left(\frac{\partial u_{z\alpha}}{\partial x}+\frac{\partial v_{z\alpha}}{\partial y}\right)\right]\frac{\partial u_{z\alpha}}{\partial x}+\left[\frac{\partial w_{z\alpha}}{\partial x}+\frac{\partial z_\alpha}{\partial x}\left(\frac{\partial u_{z\alpha}}{\partial x}+\frac{\partial v_{z\alpha}}{\partial y}\right)\right]\frac{\partial v_{z\alpha}}{\partial x}\right\}$$

(78)

and

$$\Lambda_{y2}=-\frac{1}{3}\left\{\left[\left(\zeta-z_\alpha\right)^3+\left(d+z_\alpha\right)^3\right]\left[\frac{\partial w_{z\alpha}}{\partial y}+\frac{\partial z_\alpha}{\partial y}\left(\frac{\partial u_{z\alpha}}{\partial x}+\frac{\partial v_{z\alpha}}{\partial y}\right)\right]^2\right\}_y$$
$$-\frac{1}{3}\left\{\left[\left(\zeta-z_\alpha\right)^3+\left(d+z_\alpha\right)^3\right]\left[\frac{\partial w_{z\alpha}}{\partial x}+\frac{\partial z_\alpha}{\partial x}\left(\frac{\partial u_{z\alpha}}{\partial x}+\frac{\partial v_{z\alpha}}{\partial y}\right)\right]\left[\frac{\partial w_{z\alpha}}{\partial y}+\frac{\partial z_\alpha}{\partial y}\left(\frac{\partial u_{z\alpha}}{\partial x}+\frac{\partial v_{z\alpha}}{\partial y}\right)\right]\right\}_x \tag{79}$$

Inserting Eq. (73) into the dynamic boundary condition (71) yields the *w*-momentum equation

$$\frac{\partial h w_{z\alpha}}{\partial t}+\frac{\partial h u_{z\alpha} w_{z\alpha}}{\partial x}+\frac{\partial h v_{z\alpha} w_{z\alpha}}{\partial y}-\frac{h q_{z\alpha}}{\rho\left(\zeta-z_\alpha\right)}=h w_{z\alpha}\left(\frac{\partial u_{z\alpha}}{\partial x}+\frac{\partial v_{z\alpha}}{\partial y}\right)$$
$$-h\frac{\partial z_\alpha}{\partial x}\left[w_{z\alpha}\frac{\partial w_{z\alpha}}{\partial x}+u_{z\alpha}\left(\frac{\partial u_{z\alpha}}{\partial x}+\frac{\partial v_{z\alpha}}{\partial y}\right)\right]-h\frac{\partial z_\alpha}{\partial y}\left[w_{z\alpha}\frac{\partial w_{z\alpha}}{\partial y}+v_{z\alpha}\left(\frac{\partial u_{z\alpha}}{\partial x}+\frac{\partial v_{z\alpha}}{\partial y}\right)\right]$$
$$-\frac{w_{z\alpha}}{2}\frac{\partial}{\partial x}\left\{h\left(\zeta-2z_\alpha-d\right)\left[\frac{\partial w_{z\alpha}}{\partial x}+\frac{\partial z_\alpha}{\partial x}\left(\frac{\partial u_{z\alpha}}{\partial x}+\frac{\partial v_{z\alpha}}{\partial y}\right)\right]\right\}$$
$$-\frac{w_{z\alpha}}{2}\frac{\partial}{\partial y}\left\{h\left(\zeta-2z_\alpha-d\right)\left[\frac{\partial w_{z\alpha}}{\partial y}+\frac{\partial z_\alpha}{\partial y}\left(\frac{\partial u_{z\alpha}}{\partial x}+\frac{\partial v_{z\alpha}}{\partial y}\right)\right]\right\} \tag{80}$$

Apparently, there are additional terms appeared in the right-hand side of Eq. (80), compared to Eqs. (22) and (23).

The continuity equation (73), momentum equations (74), (77) and (80), and the bottom condition (72) constitute a new set of depth-integrated nonhydrostatic equations for unknowns ζ, $u_{z\alpha}$, $v_{z\alpha}$, $w_{z\alpha}$ and $q_{z\alpha}$.

4.2 Linear and nonlinear characteristics

The linear and nonlinear second- and third-order harmonics of the new formulation may be also obtained using Stokes-type analysis as employed in Section 3.2. Collating all the terms of order $O(\varepsilon)$ leads to the linear solution and the dispersion relationship is given by

$$\omega^2=gk\frac{kd-\left(1-3\alpha+2\alpha^2\right)/2\cdot k^3d^3}{1+\alpha\left(1-\alpha\right)k^2d^2} \tag{81}$$

The velocities and nonhydrostatic pressure are respectively

$$U^{(1)}=a^{(1)}\omega\frac{2}{2kd-\left(1-\alpha\right)\left(1-2\alpha\right)k^3d^3} \tag{82}$$

$$W^{(1)}=a^{(1)}\omega\frac{2\left(1-\alpha\right)}{2-\left(1-3\alpha+\alpha^2\right)k^2d^2} \tag{83}$$

$$P^{(1)} = -\rho g a^{(1)} \frac{\alpha(1-\alpha)k^2d^2}{1+\alpha(1-\alpha)k^2d^2} \tag{84}$$

An optimized value of α for the range $0< kd \leq \pi$ may be obtained by minimizing the relative error of the phase speed over the entire range, leading to α = ½. This corresponds to the velocity defined at elevation z_α = -0.5d. The optimized dispersion relationship of (81) becomes Eq. (32). This indicates that the nonhydrostatic model with depth-integrated velocities or variables defined at the middle depth provides more accurate linear properties. This may explain why the one-layer depth-integrated nonhydrostatic model can accurately predict linear waves.

The higher-order solutions may also be obtained by collating all of the $O(\varepsilon^2)$ and $O(\varepsilon^3)$ terms, with the second- and third-order nonlinear harmonic amplitudes given by

$$a^{(2)} = \frac{ka^{(1)2}}{4}\Big[36-6\left(13-49\alpha+36\alpha^2\right)k^2d^2+2(1-\alpha)\left(51-211\alpha+321\alpha^2-162\alpha^3\right)k^4d^4 \\ -4(1-\alpha)^3(1-2\alpha)\left(10-21\alpha+18\alpha^2\right)k^6d^6\Big]\Big[18(1-\alpha)k^3d^3-9(1-\alpha)\left(1-3\alpha+2\alpha^2\right)k^5d^5\Big]^{-1} \tag{85}$$

and

$$a^{(3)} = \frac{k^2a^{(1)3}}{16}\Big[-324+54\left(35-131\alpha+96\alpha^2\right)k^2d^2-9\left(738-3954\alpha+8502\alpha^2-8094\alpha^3+2808\alpha^4\right)k^4d^4 \\ +3(1-\alpha)\left(3048-78492\alpha+112044\alpha^2-20616\alpha^3-15984\alpha^5\right)k^6d^6+\mathrm{O}\left(k^8d^8\right)\Big]/ \\ \Big[-108(1-\alpha)^2k^6d^6+54k^8d^8(1-\alpha)^2\left(1-3\alpha+2\alpha^2\right)\Big] \tag{86}$$

Series expansion from kd = 0 yields

$$a^{(2)} = \frac{3a^{(1)2}}{4k^2d^3}\left[\frac{2}{3(1-\alpha)}-\frac{10\left(1-4\alpha+3\alpha^2\right)}{9(1-\alpha)}k^2d^2+\frac{(1-\alpha)\left(37-84\alpha+72\alpha^2\right)}{27}k^4d^4+\mathrm{O}\left(k^8d^8\right)\right] \tag{87}$$

and

$$a^{(3)} = \frac{27a^{(1)3}}{64k^4d^6}\left[\frac{4}{9(1-\alpha)^2}-\frac{2\left(32-122\alpha+90\alpha^2\right)}{27(1-\alpha)^2}k^2d^2+\frac{2\left(107-336\alpha+378\alpha^2\right)}{27}k^4d^4+\mathrm{O}\left(k^8d^8\right)\right] \tag{88}$$

When using the optimized coefficient α = ½, the above expressions become

$$a^{(2)} = \frac{3a^{(1)2}}{4k^2d^3}\left[\frac{4}{3}+\frac{5}{9}k^2d^2+\frac{13}{54}k^4d^4+\mathrm{O}\left(k^8d^8\right)\right] \tag{89}$$

and

$$a^{(3)} = \frac{27a^{(1)3}}{64k^4d^6}\left\{\frac{16}{9} + \frac{52}{27}k^2d^2 + \frac{67}{27}k^4d^4 + \mathrm{O}\left(k^8d^8\right)\right\} \tag{90}$$

Apparently, they are different from the targeted equations in (41) and (42) even for the first constant terms. The constant terms in the right hand side of the second-order solution in (89) is coincident with those in Eq. (37). The different factor of the k^2d^2 term and the arising of $O(k^4d^4)$ tern in Eq. (89) are a result of retaining the nonlinear terms that were neglected by Stelling and Zijlema (2003). The overall performance of the second-order solution to the current formulation is significantly improved when choosing α = 1/2, with the maximum error less than 45% in the current model versus that of 88% in the model of Stelling and Zijlema (2003), as shown in Figure 2.

Retaining these nonlinear terms aggravates the divergence of the third-order solutions between the current formulation and the model of Stelling and Zijlema (2003), resulting in completely different expansions in Eqs. (38) and (90). The third-order solution overestimates 7/9 of the exact solution for $kd \to 0$, which is much larger than the 1/27 overestimation predicted by the model of Stelling and Zijlema (2003). Figure 2 shows that although the error of the current third-order solution decreases with kd it is still larger than that predicted by the model of Stelling and Zijlema (2003) at $kd \leq$ 0.66. As the velocities are assumed to vary linearly in the vertical direction, their completely nonlinear interactions must contain quadratic and cubic terms. This inconsistency in the governing equations may be the main reason why the formulations retaining full nonlinear terms predict larger error in the third-order solutions, comparing with the model of Stelling and Zijlema (2003).

The nonlinear properties of the generalized model may be improved by optimizing the value of α to match the Stokes theory for $kd \to 0$, which yields α = 1/3. Expansions in (85) and (86) subsequently become

$$a^{(2)} = \frac{3a^{(1)2}}{4k^2d^3}\left[1 + \frac{34}{81}k^4d^4 + \mathrm{O}\left(k^8d^8\right)\right] \tag{91}$$

and

$$a^{(3)} = \frac{27a^{(1)3}}{64k^4d^6}\left[1 - \frac{2}{9}k^2d^2 + \frac{74}{27}k^4d^4 + \mathrm{O}\left(k^8d^8\right)\right] \tag{92}$$

Apparently, the optimization gives constant terms in (91) and (92) that are identical to those in the targeted solutions in (41) and (42). Figure 2 shows improved accuracy in

the second- and third-order solutions with α = 1/3, in comparison with the model of Stelling and Zijlema (2003). The current generalized formulation with α = 1/3 provides the second-order solution with a maximum error of 30% for $kd \leq 2.55$ and the third-order solution with a maximum error of 31.5% for $kd \leq 2.47$, which are much improved compared with the model of Stelling and Zijlema (2003) and those results with α = 1/2. However, we must emphasize that the improvement of the nonlinear properties comes at a price of significantly decreasing the accuracy in linear dispersion, as shown in Figure 1. With α = 1/3, the current formulation has a phase speed error within 5% for $kd \leq 1.26$, and the error increases rapidly beyond that.

Applying a similar procedure as described in the previous section the shoaling coefficient can be obtained from Eq. (47)

$$s = \begin{bmatrix} 4-2\left(5-11\alpha+8\alpha^2\right)k^2d^2+2\left(3-15\alpha+32\alpha^2-32\alpha^3+12\alpha^4\right)k^4d^4 \\ -\left(1-\alpha\right)^3\left(4-15\alpha+22\alpha^2-16\alpha^3\right)k^6d^6-\left(1-\alpha\right)^3\alpha\left(2-10\alpha+19\alpha^2-16\alpha^3+4\alpha^4\right)k^8d^8 \end{bmatrix} \cdot \begin{bmatrix} 16-32\left(1-3\alpha+2\alpha^2\right)k^2d^2+16\left(1-\alpha\right)^2\left(1-5\alpha+6\alpha^2\right)k^4d^4 \\ +16\alpha\left(1-\alpha\right)^2\left(1-2\alpha\right)\left(1-3\alpha+2\alpha^2\right)k^6d^6-4\alpha^2\left(1-\alpha\right)^4\left(1-2\alpha\right)^2k^8d^8 \end{bmatrix}^{-1} \quad (93)$$

The shoaling coefficients corresponding to different values of α are compared with that obtained for the model of Stelling and Zijlema (2003) in Figure 3. With α = 1/2, the current formulation starts to diverge monotonically from the exact solution at kd = 2.0 and such a larger shoaling gradient will inevitably lead to overestimation of wave amplitude. Yet, the current formulation has an overall improved shoaling performance than the model of Stelling and Zijlema (2003). The possible reason is that the bottom condition (8) is described with the bottom velocities given in (72) rather than (25) that adopts the depth-integrated velocities. With α =1/3, the generalized formulation performs less satisfactorily in shoaling effect than both the model with α = 1/2 and the model of Stelling and Zijlema (2003). It agrees well with the exact relation for $kd \leq$ 1.0 and then deviates rapidly.

4. Conclusions

Stokes-type Fourier and shoaling analyses are carried out to examine the linear and nonlinear properties of depth-integrated nonhydrostatic models. The one-layer

depth-integrated nonhydrostatic model derived by Stelling and Zijlema (2003) is analyzed in detail. The model gives an error of less than 5% for the phase speed over the range $0 \leq kd \leq \pi$. Its shoaling coefficient approaches the solution to the Stokes linear theory with conservation of energy flux over the range $0 \leq kd \leq 1.1$ and then diverges rapidly. The second-order solution overestimates 1/3 of the exact solution at $kd = 0$, gradually converges to the exact solution until $kd = 0.72$ and then diverges monotonically after that. For the third-order solution, it overestimates 1/27 of the exact solution at $kd = 0$ and gradually converges to the exact solution until $kd = 0.14$. After that, the solution diverges rapidly from the exact solution.

To investigate the effects of neglecting advective and diffusive nonlinear terms, a generalized set of the depth-integrated nonhydrostatic formulations has been derived with the velocities and nonhydrostatic pressure defined at an arbitrary level. The corresponding dispersion characteristics are related to the location (indicated by coefficient α) where the variables are defined. It is found that $\alpha = 1/2$ yields the same dispersion relationship as that presents in the model derived by Stelling and Zijlema (2003), which gives an overall accurate result over the range $0 \leq kd \leq \pi$. Furthermore, the optimized value of α may also improve the model's shoaling effect. However, the model with $\alpha = 1/2$ does not exhibit significant improvement in terms of nonlinear properties, and its second- and third-order solutions respectively overestimate 1/3 and 7/9 of the exact solution for $kd \rightarrow 0$. This indicates that retaining the nonlinear terms neglected by Stelling and Zijlema (2003) may not significantly improve the nonlinear performance of the model.

With α optimized to 1/3, the model is found to better capture more accurately the nonlinear wave behaviors in shallow and intermediate water. However, such improvement comes at a price of reducing the model's capability in representing dispersion and shoaling properties; the model provides a satisfactory phase speed (with an error less than 5%) only when $kd \leq 1.26$ and a shoaling coefficient agreeing satisfactorily with the exact solution only for $kd \leq 1.0$.

With the optimized $\alpha = 1/3$, the model is able to capture the linear and nonlinear wave behaviors; however, it can be only applied within the range $kd \leq 1.0$. Such a limited

application range is a direct result of the assumption of linearly varying velocities and nonhydrostatic pressure in the vertical direction. The quadratic-over-depth flow kinematics may be used to extend the range of applicability of the model, which deserves further study.

Acknowledgements

This research was supported by the National Key Research and Development Program of China (No.: 2017YFC1404205), the National Natural Science Foundation of China (NO.: 51579090) and the Fundamental Research Funds for the Central Universities (NO.: 2015B15714).

References

Ahmadi, A., Badiei, P., Namin, M.M., 2007. An implicit two-dimensional non-hydrostatic model for free-surface flows. International Journal for Numerical Methods in Fluids 54 (9), 1055-1074.

Aricò, C., Lo Re, C., 2016. A non-hydrostatic pressure distribution solver for the nonlinear shallow water equations over irregular topography. Advances in Water Resources 98, 47-69.

Bai, Y., Cheung, K.F., 2013. Dispersion and nonlinearity of multi-layer non-hydrostatic free-surface flow. Journal of Fluid Mechanics 726, 226-260.

Casulli, V., Stelling, G.S., 1998. Numerical simulation of 3D quasi-hydrostatic, free-surface flows. Journal of Hydraulic Engineering-Asce 124 (7), 678-686.

Choi, D.Y., Wu, C.H., Young, C.-C., 2011. An efficient curvilinear non-hydrostatic model for simulating surface water waves. International Journal for Numerical Methods in Fluids 66 (9), 1093-1115.

Cui, H., Pietrzak, J.D., Stelling, G.S., 2014. Optimal dispersion with minimized Poisson equations for non-hydrostatic free surface flows. Ocean Modelling 81 (0), 1-12.

Fang, K., Liu, Z., Zou, Z., 2015. Efficient computation of coastal waves using a depth-integrated, non-hydrostatic model. Coastal Engineering 97 (0), 21-36.

Lu, X., Dong, B., Mao, B., Zhang, X., 2015. A two-dimensional depth-integrated non-hydrostatic numerical model for nearshore wave propagation. Ocean Modelling 96, Part 2, 187-202.

Ma, G., Shi, F., Kirby, J.T., 2012. Shock-capturing non-hydrostatic model for fully dispersive surface wave processes. Ocean Modelling 43–44 (0), 22-35.

Madsen, P.A., Sørensen, O.R., 1992. A new form of the Boussinesq equations with improved linear dispersion characteristics. Part 2. A slowly-varying bathymetry. Coastal Engineering 18 (3–4), 183-204.

Stelling, G., Zijlema, M., 2003. An accurate and efficient finite-difference algorithm for non-hydrostatic free-surface flow with application to wave propagation. International Journal for Numerical Methods in Fluids 43 (1), 1-23.

Svendsen, I.A., 2006. Introduction To Nearshore Hydrodynamics. World Scientific, Singapore.

Walters, R.A., 2005. A semi-implicit finite element model for non-hydrostatic (dispersive) surface waves. International Journal for Numerical Methods in Fluids 49 (7), 721-737.

Wei, Z., Jia, Y., 2014. Simulation of nearshore wave processes by a depth-integrated non-hydrostatic finite element model. Coastal Engineering 83 (0), 93-107.

Yamazaki, Y., Cheung, K.F., Kowalik, Z., 2011. Depth-integrated, non-hydrostatic model with grid nesting for tsunami generation, propagation, and run-up. International Journal for Numerical Methods in Fluids 67 (12), 2081-2107.

Young, C.C., Wu, C.H., 2009. An efficient and accurate non-hydrostatic model with embedded Boussinesq-type like equations for surface wave modeling. International Journal for Numerical Methods in Fluids 60 (1), 27-53.

Yuan, H., Wu, C.H., 2004. A two-dimensional vertical non-hydrostatic σ model with an implicit method for free-surface flows. International Journal for Numerical Methods in Fluids 44 (8), 811-835.

Zhu, L., Chen, Q., Wan, X., 2014. Optimization of non-hydrostatic Euler model for water waves. Coastal Engineering 91 (0), 191-199.

Zijlema, M., Stelling, G., Smit, P., 2011. SWASH: An operational public domain code for simulating wave fields and rapidly varied flows in coastal waters. Coastal Engineering 58 (10), 992-1012.

Zijlema, M., Stelling, G.S., 2005. Further experiences with computing non-hydrostatic free-surface flows involving water waves. International Journal for Numerical Methods in Fluids 48 (2), 169-197.

Figure captions

Figure 1 Comparison of normalized phase speeds.

Figure 2 Ratios of second harmonic $a^{(2)} / a^{(2)}_{\text{Stokes}}$ and third harmonic $a^{(3)} / a^{(3)}_{\text{Stokes}}$.

Figure 3 Linear shoaling gradient for the depth-integrated nonhydrostatic model of Stelling and Zijlema (2003) and the generalized one-layer formulation with different values of α.

Figure

Figure 1

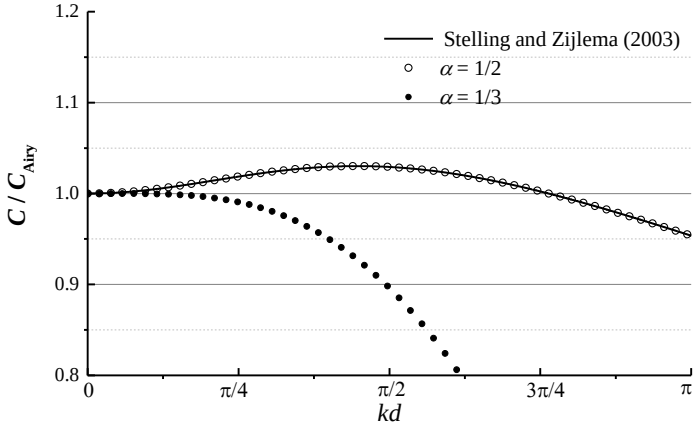

Figure 2

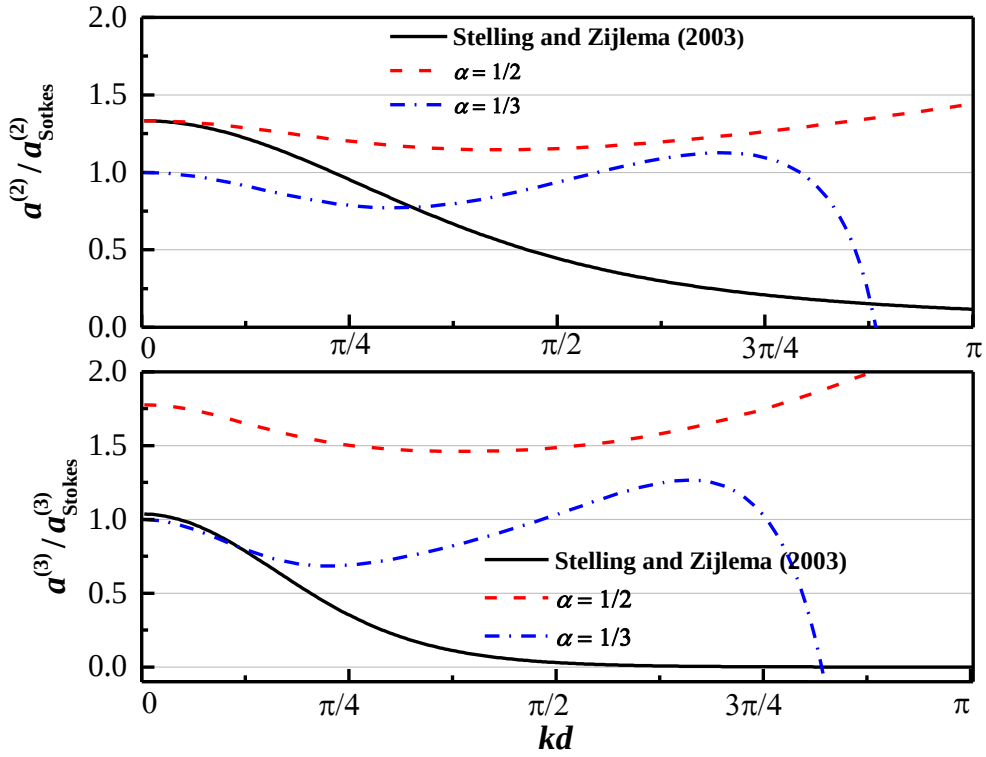
2.0
1.5
1.0
0.5
0.0
$a^{(2)}/a^{(2)}_{Sotkes}$
Stelling and Zijlema (2003)
α = 1/2
α = 1/3
0
π/4
π/2
3π/4
π
$a^{(3)}/a^{(3)}_{Stokes}$
Stelling and Zijlema (2003)
α = 1/2
α = 1/3
kd

Figure 3

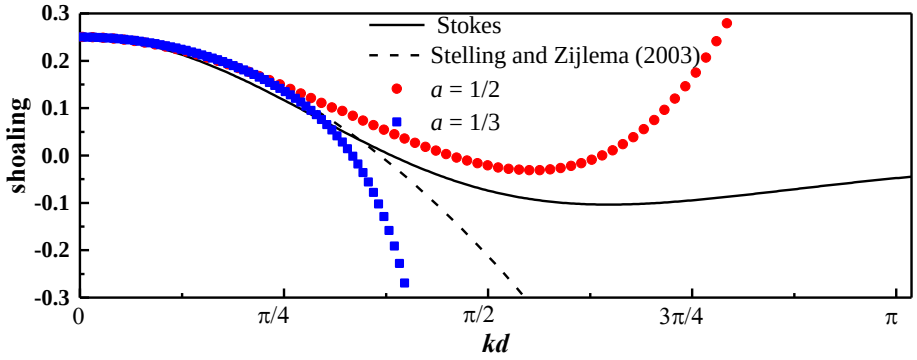
Stokes
Stelling and Zijlema (2003)
a = 1/2
a = 1/3
shoaling
0.3
0.2
0.1
0.0
-0.1
-0.2
-0.3
0
π/4
π/2
3π/4
π
kd